AGU PUBLICATIONS

Water Resources Research

TECHNICAL REPORTS: METHODS

10.1002/2014WR015847

Key Points:
- Dispersive and chromatographic mixing at oscillating interfaces is simulated
- Oscillations and nonlinear cation exchange give asymmetric fronts
- Oscillating nonlinear mixing converges to zero-convection nonlinear diffusion

Supporting Information:
- Supporting Information S1

Correspondence to:
D. G. Cirkel,
Gijsbert.cirkel@kwrwater.nl

Citation:
Cirkel, D. G., S. E. A. T. M. van der Zee, and J. C. L. Meeussen (2015), Front spreading with nonlinear sorption for oscillating flow, *Water Resour. Res.*, *51*, 2986–2993, doi:10.1002/2014WR015847.

Received 20 MAY 2014
Accepted 15 MAR 2015
Accepted article online 23 MAR 2015
Published online 23 APR 2015

Front spreading with nonlinear sorption for oscillating flow

D. G. Cirkel[1,2], S. E. A. T. M. van der Zee[2], and J. C. L. Meeussen[3]

[1]KWR Water Cycle Research Institute, Water Systems and Technology, Nieuwegein, Netherlands, [2]Wageningen University, Environmental Sciences Group, Soil Physics and Land Management, Wageningen, Netherlands, [3]NRG, Radiation and Environment, Petten, Netherlands

Abstract In this paper, we consider dispersive and chromatographic mixing at an interface, under alternating flow conditions. In case of a nonreactive or linearly sorbing solute, mixing is in complete analogy with classical dispersion theory. For nonlinear exchange, however, oscillating convective flow leads to an alternation of sharpening (Traveling Wave TW) and spreading (Rarefaction Wave RW). As the limiting TW form is not necessarily accomplished at the end of the TW half cycle, the oscillating fronts show gradual continuous spreading that converges to a zero-convection nonlinear pure diffusion spreading, which is mathematically of quite different nature. This behavior is maintained in case the total (background) concentration differs at both sides of the initial exchange front.

1. Introduction

Mixing processes at solute fronts have received considerable attention over the past decades, particularly for nonreacting solutes [*Bear*, 1972; *De Josselin de Jong*, 1958]. Reactive transport is mathematically more complicated if the reactions are nonlinear in concentration [*Bolt*, 1982; *Levenspiel*, 1972]. Whereas 1D situations (chemical reactors in industry, vertical displacement in the vadose zone) were emphasized, multi-D and heterogeneous systems were also considered [*Bellin et al.*, 1993; *Cirpka and Kitanidis*, 2000; *Janssen et al.*, 2006; *Prommer et al.*, 2003; *Tang et al.*, 1981].

Modest attention has been given to situations where a concentration front position fluctuates as a function of time, instead of a monotonous displacement in one direction, despite the practical relevance of e.g., aquifer thermal energy storage [*Bonte et al.*, 2011; *Gao et al.*, 2009; *Zuurbier et al.*, 2013] and fresh water lenses [*Eeman et al.*, 2012]. The effect of oscillating concentration fronts has received relatively little attention to our knowledge [e.g., *Raats*, 1969, 1973], particularly reactive cases.

In this paper, we consider dispersive and chromatographic mixing at an interface, of which the mean depth varies periodically as a function of time, in particular for Gapon cation exchange, as an example of nonlinear chemical interactions, for the case that the total salt concentration is either constant or not.

2. Theory

2.1. Basic Equations

We consider a nonreactive and a nonlinear exchange case, respectively. Gapon cation exchange between a monovalent cation, sodium (Na) and a divalent cation, calcium (Ca), is described by

$$\frac{q_{Na}}{q_{Ca}} = K_G \cdot \frac{c_{Na}}{\sqrt{c_{Ca}/2}}, \tag{1}$$

where concentrations in solution c, are conventionally in mol_c/dm^3. Mol_c stands for mol charge. And q, is the adsorbed concentration (also mol_c/dm^3). We normalize as follows:

$$\bar{c} = \frac{c - c_i}{c_f - c_i} = \frac{f - f_i}{f_f - f_i}, \bar{q} = \frac{q - q_i}{q_f - q_i} = \frac{N - N_i}{N_f - N_i}$$

and rewrite equation (1):

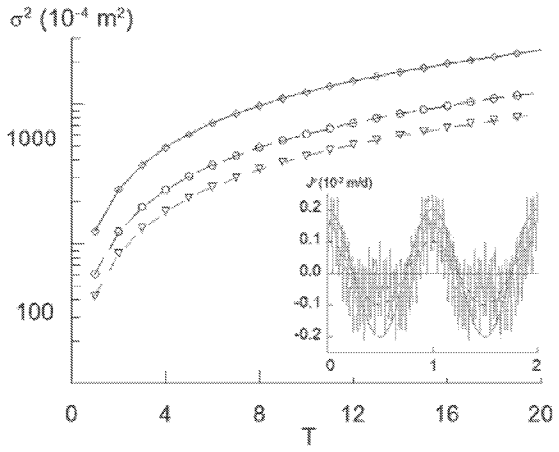

Figure 1. Increase of the mixing zone width (second central moment of the concentration gradient) as a function of time. Numerical (lines) and analytical approximation $\sigma = \sqrt{2\alpha < |v| > t}$. Data for two cosine flow rate functions (amplitudes 0.1×10^{-2} (circles), 0.2×10^{-2} m/d (diamonds), and an irregular function (triangles).

$$\frac{1-N}{N} = K_G\sqrt{2C}\cdot\frac{1-f}{\sqrt{f}}, \tag{2}$$

where the fractions are given by:

$$f=\frac{c_{Ca}}{C};\ 1-f=\frac{c_{Na}}{C};\ N=\frac{q_{Ca}}{\varepsilon_c};\ 1-N=\frac{q_{Na}}{\varepsilon_c}$$
$$\text{and } C=c_{Na}+c_{Ca}. \tag{3}$$

in which (capital) C is the total concentration (sum of all cations or of all anions) and ε_c is the cation exchange capacity, CEC in mol_c/dm^3. Considering only two cations, we can eliminate one (sodium Na) and rewrite N as a function of f: $N(f)$.

We obtain the mass balance equation in terms of f, for 1D transport in direction x as:

$$\frac{\partial}{\partial t}\left[\varepsilon_c N(f)+nCf\right]+\frac{\partial}{\partial x}\left[J^v Cf\right]=\frac{\partial}{\partial x}nD\left[\frac{\partial Cf}{\partial x}\right], \tag{4}$$

where q is the specific discharge in m/d and $J^v = v \cdot n$ if n = water filled porosity), D is the dispersion coefficient (m^2/d), t is time, and we neglect molecular diffusion. Following *Bear* [1972], we have:

$$D=\alpha|v|. \tag{5}$$

Combining equations (4) and (5) yields for constant C:

$$\frac{\partial}{\partial t}\left[\varepsilon_c^* \cdot N(f)+f\right]+\frac{\partial}{\partial x}[vf]=\frac{\partial}{\partial x}D\left[\frac{\partial f}{\partial x}\right], \tag{6}$$

with $\varepsilon_c^* = \frac{\varepsilon_c}{nC}$, which is the ratio of (adsorbed and dissolved) pool sizes.

For the pore water velocity, v, we assume $v = v_A\cos(\omega t)$.

We consider alternative ways for fluctuating v-values, see Figure 1, for the nonreactive solute. For $t = T$ we have a full cycle ($T = 2\pi/\omega$), an average velocity $<v> = \frac{1}{T}\int_0^T v(s)ds = \frac{v_A}{T}\int_0^T \cos(\omega s)ds = 0$ and the average absolute velocity $<|v|> = \frac{1}{T}\int_0^T |v(s)|ds = \frac{v_A}{T}\int_0^T |\cos(\omega s)ds| = \frac{2v_A}{T}$

2.2. Nonreactive Solute Transport

If $K_G = 0$, equation (6) becomes

$$\frac{\partial}{\partial t}[f]+\frac{\partial}{\partial x}[vf]=\frac{\partial}{\partial x}D\left[\frac{\partial f}{\partial x}\right] \tag{7}$$

If we average over a complete cycle, we find a dispersion term just as *Raats and Scotter* [1968]:

$$<\frac{\partial}{\partial x}D\left[\frac{\partial f}{\partial x}\right]> = \frac{1}{T}\int_0^T \frac{\partial}{\partial x}\left[\alpha|v_A\cos(\omega s)|\frac{\partial f}{\partial x}\right]ds = \frac{\alpha v_A}{T}\int_0^T |\cos(\omega s)ds|\frac{\partial^2 f}{\partial x^2} = \alpha <|v|> \frac{\partial^2 f}{\partial x^2}, \tag{8}$$

provided that the time dependency of the derivative term (the gradient) may be neglected. This approximation appears to be valid (see S1). For the nonreactive case, the width of the mixing zone in the Fickian regime, can be parameterized by the standard deviation, σ, (or variance, σ^2) of this zone

$$\sigma = \sqrt{2\alpha <|v|> t} \tag{9}$$

and the mean absolute velocity equals the traveled distance over total time (i.e., not the "effective" distance, which is zero). For a constant velocity, this result is well-known *Bear* [1972], *Dagan* [1989]. The perfect agreement for oscillating flow (cosine flow rate irregular functions) is shown in Figure 1 and agrees with conclusions of *Scotter and Raats* [1968]. As both our results and *Eeman et al.* [2012] show, the excellent agreement is maintained for highly irregular variations in interface velocity e.g., as derived from real rainfall records. As on the longer term, the net interface displacement of the interface is zero, a zero-convection diffusion equation describes the mixing at the interface.

2.3. Reactive Solute Transport

Sorption nonlinearity affects the front shape (or, for constant total concentration, the concentration fraction f) in two ways. A traveling wave develops if either one of the following conditions is met: $f_0 > f_i, \frac{dN(f)}{df} > 0, \frac{d^2N(f)}{df^2} < 0$ or $f_0 < f_i, \frac{dN(f)}{df} > 0, \frac{d^2N(f)}{df^2} > 0$ [*Van der Zee*, 1990]. Where the constraints of Van der Zee has been translated from C and $f(C)$ into f and $N(f)$, respectively, and where subscript i stands for initial resident and 0 for feed solution. If the constraint are not met, dispersional spreading of the front is enhanced by this nonlinearity and a rarefied/rarefaction wave (RW) develops. For the TW case, an analytical solution is available for the limiting front (t approaching ∞) for Gapon exchange $N(f)$ [*Bolt*, 1982; *Reiniger and Bolt*, 1972].

2.3.1. RW Behavior

We first assume that $D = 0$, yielding:

$$\frac{\partial}{\partial t}\left[\varepsilon_c^+ N(f)+f\right]+\frac{\partial}{\partial x}[vf]=0. \tag{10}$$

A Rarefaction Wave (RW) regime is found, if f increases in the direction of flow for Gapon exchange. If f decreases in the direction of flow, a shock develops positioned according to mass balance considerations. The hyperbolic equations for the RW can be described with the Method of Characteristics, and for an initial step front at some $x=0$, we obtain:

$$x_c=\frac{vt}{1+\frac{\varepsilon_c\sqrt{C}(f+1)K_G}{Cn\sqrt{2}\sqrt{f}\left(-\sqrt{2}\sqrt{C}fK_G+\sqrt{2}\sqrt{C}K_G+\sqrt{f}\right)^2}}, \tag{11}$$

using the chain rule.

In case $D > 0$, the RW case can be corrected according to *Bolt* [1982], using $\delta_f=2\sqrt{(\alpha vt)}inverfc(2f)$, where the position of each f-value is corrected with a factor that follows from the nonreactive transport solution.

If the concentration fraction f decreases in the direction of flow and the criteria are met, a Traveling Wave (TW) develops. Analytical solutions were developed for Gapon by *Bolt* [1982], and for other cases by *Van der Zee* [1990]. For Gapon exchange, we use a solution of the type: $\breve{x}=x-v^*t+u$ and $S\breve{x}/\alpha=F(f)$, that slightly differs from that of *Bolt* [1982] (see supporting information Figure S2).

3. Results for Gapon Exchange

3.1. Unidirectional Flow

To appreciate how appropriate the approximations of the previous section are, we modeled transport for a constant flow rate, using Orchestra [*Meeussen*, 2003]. The agreement between numerical and analytical results of Figure 2 for RW and TW is good to excellent. For RW, ignoring the ad hoc correction for dispersion (solid lines) leads to more appreciable discrepancies. To avoid discretization errors, as discussed for Freundlich adsorption by *Bosma and van der Zee* [1993], a node distance Δx was chosen of 1.0×10^{-3} m for the TW case. The water-filled porosity n, density ρ, kg m^{-3}, dispersivity α, m and cation exchange capacity ε_c, mol$_c$ kg^{-1} were kept constant during our analysis at, respectively, 0.38, 1650, 0.005, and 0.0125.

3.2. Oscillating Fronts

For oscillating fronts, we assume a cosine-shaped-specific discharge, q with amplitude of 0.1×10^{-2} m d^{-1} and a period T of 1 year. As initial condition, a step front at $x = 200$ cm, separates the initial calcium concentration c_i of 2.000×10^{-5} at small x-values from the calcium concentration in the feed solution c_f of 2.001×10^{-2} mol$_c$ dm^{-3} for larger x-values. As Gapon exchange depends on the total cation concentration, C, (equation (1)), the total concentration was kept constant throughout the column at 2.002×10^{-2} mol$_c$

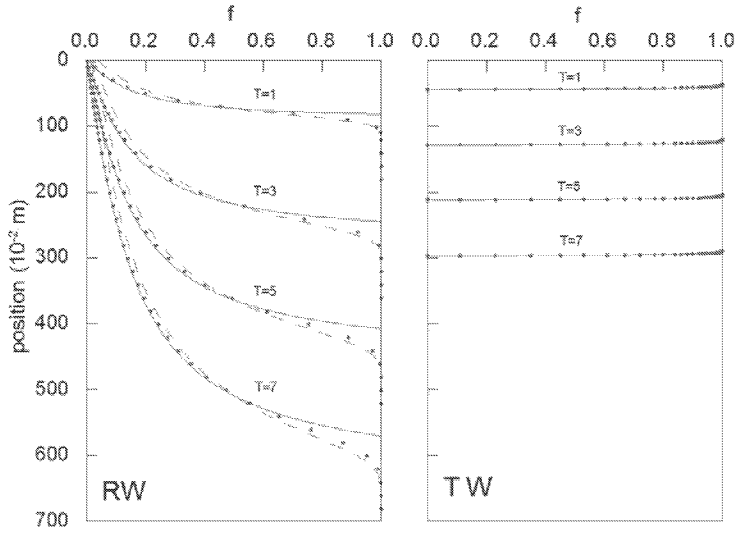

Figure 2. Agreement between (left: RW) numerical (dots) and the analytical RW approximations without (solid lines; equation (11)) and with correction factor for dispersion (dashed line), and (right: TW) numerical (dots) and analytical TW solution (solid lines). Both with $J' = 0.1 \times 10^{-2}$ m d^{-1}.

dm^{-3}. We show results for $f(x, t^*)$ (equation (3)), at specific times where the initial position (beginning of cycle, front moving downward), the lowest position, the highest position, and the intermediate one (front moving upward or downward) are attained (see Figure 3).

The front shapes (Figure 3, left) at the highest and lowest positions differ. As the front moves from the initial step front to the lowest position (a), a rather sigmoid front results, where adsorption and dispersion enhance front spreading in the RW regime. For the highest position (c), conversely, a steep front is found, which, in view of the nonlinearity and initial/boundary conditions, shows TW behavior. When we shift the flow cycle by half a period, moving first from the initial step front upward (Figure 3, right figure), the cycle starts with TW behavior (a'), changes to RW behavior (b', c') and ends with TW behavior (d').

The front shape at position c, that follows after a RW phase is less sharp than the shape at a' that follows from a step front. The sharpening behavior is also visible in the transition from the front at position b to position c (Figure 3, left figure). Reminding that the analytical solution for the TW phase represents a limiting front, these differences emphasize that self-sharpening takes time (which is not sufficiently available during the cycles). As the number of cosine-cycles grows, the numerical fronts therefore continue to flatten and cover an increasingly larger x-range. Interestingly, the front shapes of the "intermediate positions" (b, d) are rapidly becoming identical for the moving upward and for the moving downward phase of the cosine-shaped velocity cycle (Figure 4).

As the deviation of the starting front (e.g., our initial step front, or, after some cycles, a RW front) from the limiting TW becomes larger, the time to attain the limiting front closely enough also becomes larger. Our results indicate that the convergence rate is too slow to attain the limiting TW, hence, in each following RW phase, we observe rapid further spreading due to nonlinearity and hydrodynamic dispersion, and with each next cycle, the limiting TW is approached less well. The spreading behavior of the convective oscillating fronts is maintained at different amplitudes J'_A of the cosine-velocity cycles, different values for ε_c, and different values for K_G (supporting information Figure S2). Therefore, all evidence points to a systematical discrepancy between RW spreading and TW sharpening, where the overall effect is that of continued spreading!

3.3. Nonlinear Diffusion

For constant unidirectional velocity, the analytical (TW and RW) solutions provided a very good approximation. For both cases, convection is essential. This implies that nonlinear diffusion, i.e., in our case purely diffusive zero-convection transport and exchange that is nonlinear with respect to solute concentrations, is essentially different from the convective dispersive transport involving interface oscillations. As with an

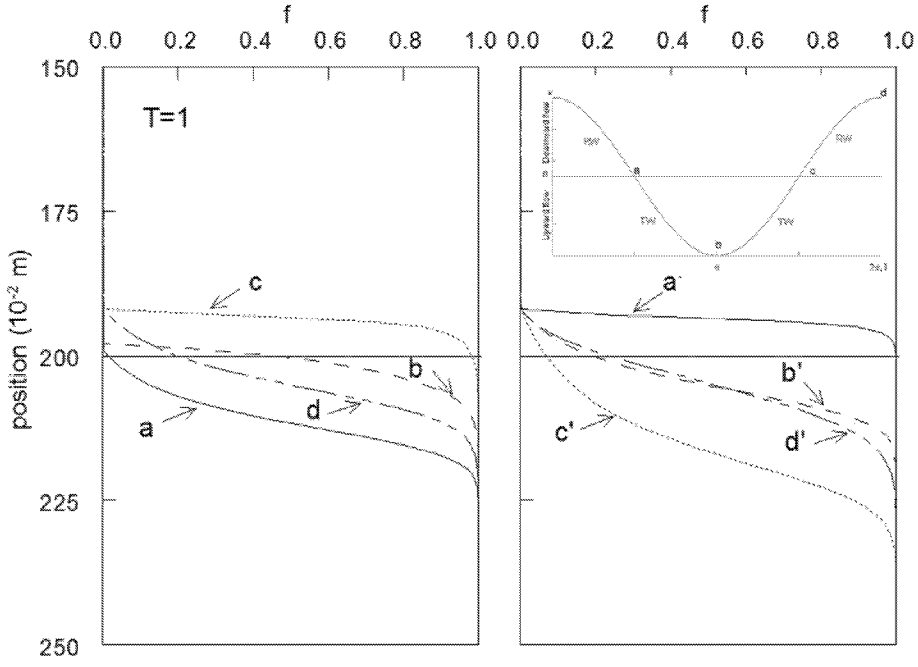

Figure 3. Solute fronts during the first cosine velocity cycle. (left) Solute fronts (bivalent ions) at positions a, b, c and d if starting at t=0 in downward direction. (right) Same but starting in upward direction.

increasing number of cosine-cycles, the fronts deviate from both TW and RW solutions and behavior, it is conceivable that on the longer term (many cycles), the overall spreading of the front is comparable to that of a pure (nonlinear) diffusion equation, e.g., as analyzed by *Van Duijn and Peletier* [1977]. For this reason, we compared a pure nonlinear diffusion front with adjusted diffusion coefficient, with a long-term front with oscillating flow in Figure 5. The diffusion front with zero convection, corresponds well with the positions b and d of the oscillating convective-dispersive case. To test the agreement with nonlinear diffusion, with adjusted value of D, we used spatial moments rather than a coarse visual inspection of front shapes [*Bosma and van der Zee*, 1993]. The spatial moments mean (μ), variance (σ^2), skewness (γ_1), and kurtosis (γ_2) were calculated for each of the four positions of the oscillating case and for the diffusive case according to *Janssen et al.* [2006]. For convenience, we did so for the concentration fraction (f) instead of mass as the water content is kept constant during our analysis. From the nonreactive case, we approximate the effective diffusion coefficient D_e by: $D_e \approx \alpha < |v| >$. The mean position of the diffusion front (solid line) agrees well with the mean position of the intermediate fronts (b and d) (circles, diamonds) of oscillating flow (Figure 5). Moreover, kurtosis and skewness of the intermediate fronts (b and d) also converge to the values of the pure diffusive front after approximately 20 cosine cycles. The variance of the diffusion front shape slightly deviates from the intermediate positions (b and d), but reflects the "upper" position (c) very well. After many cosine cycles, the relative deviations between oscillating convective dispersive mixing and nonlinear diffusion are small. Based on our analysis, it thus appears that mixing as a result of oscillating flow approaches a nonlinear diffusion (zero convection) equation, with an effective diffusion coefficient D_e based on the product of the absolute average movement of the interface $<|v|>$ and the dispersivity α. As mentioned, the diffusive spreading behavior is maintained at different parameter values.

3.4. Effect of A Salinity Front

So far, we assumed a constant total concentration (C) throughout the domain. To test the effect of a salinity front, where this is not the case, we reduced the total concentration C above the step front with a factor 10 from 2.002×10^{-2} to 2.002×10^{-3} mol_c dm^{-3} and concentrations of the bivalent and monovalent cations are scaled accordingly.

The basic concentration fronts for total concentration or Cl, Ca, and Na, are shown in Figure 6(left). The Na and Ca concentration fronts are normalized by the maximum concentration in the system. The total

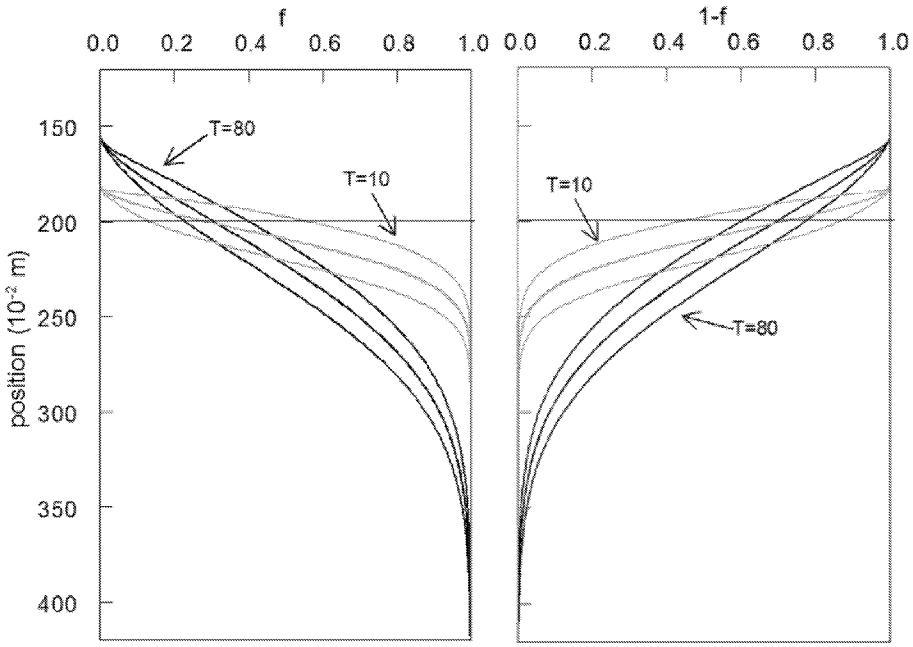

Figure 4. Solute fronts for velocity cycle T = 10 and T = 80. Left: divalent cations (Ca), right monovalent cations (Na). Fronts for divalent f and monovalent 1-f cations are complements (mirror image), due to equation (3) and constant total concentration.

concentration or Cl fronts are normalized using c/c_{min}, for easy comparison with the shape of the Na concentration fronts. Also shown are Ca and Na expressed as concentration fractions f and $1-f$. Compared to the previously shown Ca fronts, the current normalized Ca fronts are only slightly influenced by the salinity front, but show less spreading. Expressed as dimensionless fraction f, these differences become more apparent (Figure 7). The fronts in case of a salinity front are sharper and move slightly faster in the direction of

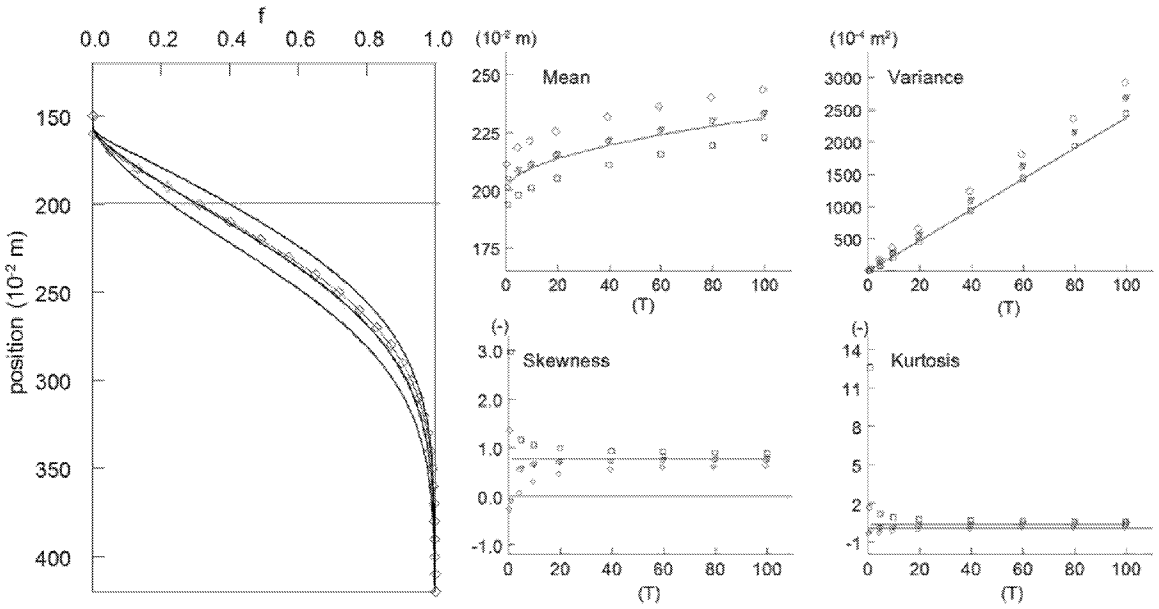

Figure 5. Comparison of front shapes at cycle T= 80 (lines) for oscillating flow with front shape at T=80 calculated with diffusion only (diamonds) and (right) spatial moments for oscillating convective-dispersive and pure diffusion (zero convection: lines) fronts for divalent cations. Symbols: values for positions of inset Figure 2: a (diamonds), b (circles), c (squares), and d (triangles).

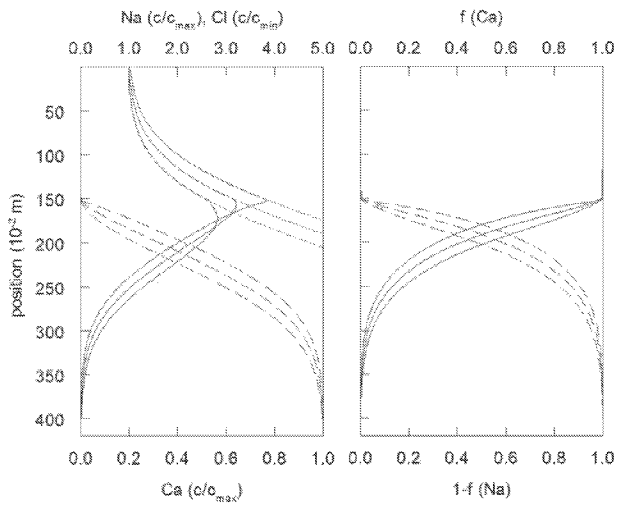

Figure 6. Concentration profiles for the case of a change in total concentration at T=80. (left) Concentration profiles, presented as c/c_{max} for Na (solid line) and Ca (dashed line) and as c/c_{min} for Cl (partly shown with dotted line) in case of a change in total concentration C (salinity front). (right) Position and shape of the solute fronts, expressed as concentration fractions f (Ca) (dashed line) and $1-f$ (Na) (solid line).

lower total concentration. The sharpness of the front is in accordance with the higher affinity of the cation exchange complex (hence, stronger nonlinearity) for Ca at lower total concentrations. The faster movement of the front is perhaps a bit counterintuitive at first glance, in view of the higher affinity. However, exactly because of this higher affinity for Ca, the initial amount of adsorbed Ca for smaller z-values is larger in case the total concentration there is smaller: $N=0.5$ instead of 0.23. This implies, on the basis of a simple mass balance consideration, that the front moves faster if the upper total concentration is decreased.

The total concentration (expressed by chloride) front (partly shown in Figure 6) agrees with classical (symmetric) Fickian spreading. The distance over which this front extends is larger than for the calcium front and equal to that of sodium. For sodium, though, a concentration peak occurs that is larger than the initial concentration on either side of the initial shock front. Such peaks are due to the combination of change in total concentration and nonlinear exchange between calcium and sodium. The peak concentration for sodium coincides with the maximum position of the calcium front. As can be seen from Figure 6, the concentration from this position to smaller numbers is controlled completely by the Fickian spreading of the total concentration front. The sodium concentration from position 150 to higher numbers is controlled by both spreading of the total concentration front and (nonlinear) exchange depending on the shape of the exchange isotherm and the direction of flow.

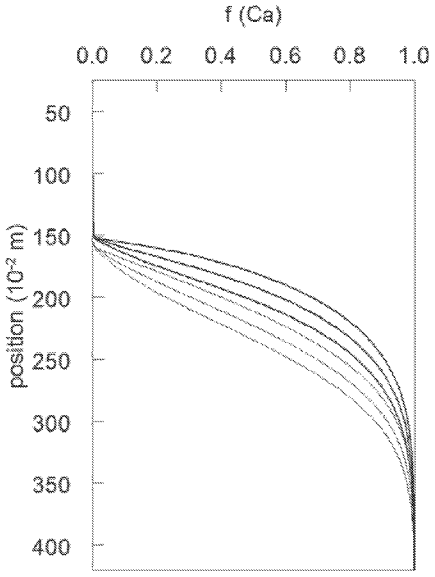

Figure 7. Comparison of front shapes for f with (thick lines) and without (thin lines) a change in total concentration C (salinity front). Data shown for velocity cycle T=80.

4. Conclusions

We conclude that from the nonreactive case, an approximation for the effective dispersion coefficient can be derived, that holds also for irregular fluctuations, in magnitude and direction, of the flow velocity.

In case of nonlinear exchange in combination with alternating flow, the solute front continues to spread, which indicates that the approach to a traveling wave during part of the displacement is insufficient to reach the limiting front. Accordingly, the continuously spreading front seems to approach a nonlinear diffusion

front, with adjusted dispersion coefficient and zero convection, and which is mathematically of quite different nature. Allowing for a total concentration change, spreading is somewhat affected in magnitude.

Acknowledgments
This study was carried out within the framework of the NWO CASIMIR programme (018.002.007), Dutch Water Utility Sector joint research programme (BTO) and Knowledge for Climate programme (Theme 2 and 3). We appreciated discussions in the NUPUS network and suggestions of A. Leijnse. Data are made available upon request from the authors (Gijsbert.cirkel@kwrwater.nl).

References

Bear, J. (1972), *Hydraulics of Groundwater*, 569 pp., McGraw-Hill, N. Y.
Bellin, A., A. Rinaldo, W. J. P. Bosma, S. E. A. T. M. van der Zee, and Y. Rubin (1993), Linear equilibrium adsorbing solute transport in physically and chemically heterogeneous porous formations: 1. Analytical solutions, *Water Resour. Res.*, *29*(12), 4019–4030.
Bolt, G. H. (1982), *Soil Chemistry. B. Physico-Chemical Models*, 459 pp., Elsevier, Amsterdam, Netherlands.
Bonte, M., P. J. Stuyfzand, G. A. van den Berg, and W. A. Hijnen (2011), Effects of aquifer thermal energy storage on groundwater quality and the consequences for drinking water production: a case study from The Netherlands, *Water Sci. Technol.*, *63*(9), 1922–1931.
Bosma, W. J. P., and S. E. A. T. M. van der Zee (1993), Transport of reacting solute in a one-dimensional, chemically heterogeneous porous medium, *Water Resour. Res.*, *29*(1), 117–131.
Cirpka, O. A., and P. K. Kitanidis (2000), Characterization of mixing and dilution in heterogeneous aquifers by means of local temporal moments, *Water Resour. Res.*, *36*(5), 1221–1236.
Dagan, G. (1989), *Flow and Transport in Porous Media*, 465 pp., Springer, N. Y.
De Josselin de Jong, G. (1958), Longitudinal and transverse diffusion in granular deposits, *Trans. AGU 39*, 67–74.
Eeman, S., S. E. A. T. M. van der Zee, A. Leijnse, P. G. B. de Louw, and C. Maas (2012), Response to recharge variation of thin rainwater lenses and their mixing zone with underlying saline groundwater, *Hydrol. Earth Syst. Sci.*, *16*(10), 3535–3549.
Gao, Q., M. Li, M. Yu, J. D. Spitler, and Y. Y. Yan (2009), Review of development from GSHP to UTES in China and other countries, *Renew. Sustain. Energy Rev.*, *13*(6–7), 1383–1394.
Janssen, G. M. C. M., O. A. Cirpka, and S. E. A. T. M. van der Zee (2006), Stochastic analysis of nonlinear biodegradation in regimes controlled by both chromatographic and dispersive mixing, *Water Resour. Res.*, *42*, W01417, doi:10.1029/2005WR004042.
Levenspiel, O. (1972), *Chemical Reaction Engineering*, 578 pp., John Wiley, N. Y.
Meeussen, J. C. L. (2003), ORCHESTRA: An object-oriented framework for implementing chemical equilibrium models, *Environ. Sci. Technol.*, *37*(6), 1175–1182.
Prommer, H., D. A. Barry, and C. Zheng (2003), MODFLOW/MT3DMS-based reactive multicomponent transport modeling, *Ground Water*, *41*(2), 247–257.
Raats, P. A. C. (1969), The effect of a finite response time upon the propagation of sinusoidal oscillations of fluids in porous media, *Z. Angew. Math. Phys.*, *20*(6), 936–946.
Raats, P. A. C. (1973), Propagation of sinusoidal solute density oscillations in the mobile and stagnant phases of a soil1, *Soil Sci. Soc. Am. J.*, *37*(5), 676–680.
Raats, P. A. C., and D. R. Scotter (1968), Dynamically similar motion of two miscible constituents in porous mediums, *Water Resour. Res.*, *4*(3), 561–568.
Reiniger, P., and G. H. Bolt (1972), Theory of chromatography and its application to cation exchange in soils, *Neth. J. Agric. Sci.*, *20*, 301–313.
Scotter, D. R., and P. A. C. Raats (1968), Dispersion in Porous Mediums Due to Oscillating Flow, *Water Resour. Res.*, *4*(6), 1201–1206.
Tang, D. H., E. O. Frind, and E. A. Sudicky (1981), Contaminant transport in fractured porous media: Analytical solution for a single fracture, *Water Resour. Res.*, *17*(3), 555–564.
Van der Zee, S. E. A. T. M. (1990), Analytical traveling wave solutions for transport with nonlinear and nonequilibrium adsorption, *Water Resour. Res.*, *26*(10), 2563–2578.
Van Duijn, C. J., and L. A. Peletier (1977), A class of similarity solutions of the nonlinear diffusion equation, *Nonlinear Anal. Theory, Methods Appl.*, *1*(3), 223–233.
Zuurbier, K. G., N. Hartog, J. Valstar, V. E. A. Post, and B. M. van Breukelen (2013), The impact of low-temperature seasonal aquifer thermal energy storage (SATES) systems on chlorinated solvent contaminated groundwater: Modeling of spreading and degradation, *J. Contam. Hydrol.*, *147*(0), 1–13.